Engineering Structures 33 (2011) 2603–2611

Contents lists available at ScienceDirect

Engineering Structures

journal homepage: www.elsevier.com/locate/engstruct

Form finding methodology for force-modelled anticlastic shells in glass fibre textile reinforced cement composites

Tine Tysmans [a,*], Sigrid Adriaenssens [a,b], Jan Wastiels [a]

[a] Vrije Universiteit Brussel, Faculty of Engineering Sciences, Department of Mechanics of Materials and Constructions (MeMC), Pleinlaan 2, B-1050 Brussels, Belgium

[b] Princeton University, Department of Civil and Environmental Engineering, E-Quad E332, Princeton, NJ 08544, USA

ARTICLE INFO

Article history:
Received 10 August 2010
Received in revised form
19 January 2011
Accepted 2 May 2011
Available online 11 June 2011

Keywords:
Cement composites
Dynamic relaxation
Form finding
Glass fibres
Textile reinforcement
Shells

ABSTRACT

The reinforcement of a specifically developed fine grained cement matrix with glass fibre textiles in high fibre volume fractions creates a fire safe composite that has – besides its usual compressive strength – an important tensile capacity and omits the need for any steel reinforcement. Strongly curved shells made of textile reinforced cement composites (TRC) can cover medium (up to 15 m) span spaces with three times smaller shell thicknesses than conventional steel-reinforced concrete shells. This paper presents a methodology to generate force-modelled anticlastic shell shapes that exploit both the tensile and compressive load carrying capacities of TRC. The force-modelling is based on the dynamic relaxation form finding method developed for gravity (in this case self-weight) loaded systems. The potential of the presented methodology to develop structurally sound anticlastic shell shapes is illustrated by four case studies.

1. Introduction

The research presented in this paper addresses the renewed design interest in complex curved structural surfaces. After a period of blooming in the 1950s and 1960s with shell builders such as Candela and Isler, the realisation of thin reinforced concrete shells reduced drastically in the 1970s, mainly because of the increase in construction costs [1,2]. Recent advances in textile formwork and composite technology have the potential to make shells economically competitive and lead to innovative shell applications.

Extensive research by West [3], Pronk et al. [4], the Belgian Building Research Institute [5] and Guldentops et al. [6] demonstrates the theoretical as well as practical feasibility of form active shell moulding. Synclastic shells, or domes, can easily be produced with inflated membranes. The force-efficiency of a gravity loaded shell shape, obtained with an inflated membrane under pressure, is limited to shallow domes [7]. Anticlastic concrete shells, however, can be constructed with minimum labour costs on a pre-stressed membrane without slope or curvature restrictions. This technique is particularly economical with re-usable membranes.

The construction of anticlastic shells with high curvature can be even more facilitated through the use of flexible fibre reinforcement. Cement-based composites offer a fire safe alternative for fibre reinforced polymers to construct curved shapes, but are limited in fibre volume fraction when short fibres are used in a premix system, as is usually the case. The use of continuous fibre systems, called textiles [8,9], allows the impregnation of much higher fibre volume fractions if the grain size and rheology of the cement matrix is adapted to the high density of the textile [8]. Researchers at the Vrije Universiteit Brussel developed a fine grained cement matrix, Inorganic Phosphate Cement, that can impregnate dense glass fibre textiles up to 20% fibre volume fraction and more [10], resulting in a high tensile capacity while making any other reinforcement, like steel, redundant. The thickness of noncorroding Glass fibre Textile Reinforced Inorganic Phosphate Cement (GTR-IPC) shells is no longer restricted by corrosion cover regulations, in contrast with the minimum 70 mm thickness for steel-reinforced concrete shells required by Eurocode 2 [11]. GTR-IPC shells can be made as thin as structurally necessary. This fact makes these shells economical in material use for smaller applications. Previous research [12,13] has proven that the application of GTR-IPC to medium span (up to 15 m) shells leads to a considerable thickness reduction in comparison with steel-reinforced concrete.

This paper focuses on an important aspect of anticlastic GTR-IPC shell design: the determination of a force-efficient initial shell geometry. The choice for strongly curved, anticlastic shell shapes does not only take into account the facilitated manufacturing on a pre-stressed membrane, but most of all exploits the most advantageous property of GTR-IPC to carry tensile as well as compressive stresses. With this cement composite, innovative anticlastic shell shapes can be designed that hold the synergy between

* Corresponding author. Tel.: +32 2 6292921; fax: +32 2 6292928.
E-mail address: ttysmans@vub.ac.be (T. Tysmans).

0141-0296/$ – see front matter © 2011 Elsevier Ltd. All rights reserved.
doi:10.1016/j.engstruct.2011.05.007

small, anchored anticlastic membrane structures and strongly reinforced, large span, anticlastic concrete shells. These anticlastic GTR-IPC shells carry distributed loads by two perpendicular line systems of catenaries curved in opposite directions, which are each effective in resisting any change in the shape of the other [14], and hereby increase significantly the shell's resistance to buckling. The intrinsically high buckling resistance of the anticlastic shape is an important advantage for the envisioned applications of very thin GTR-IPC shells built on a membrane formwork, a manufacturing process during which deformations of the order of magnitude of the shell's thickness commonly occur. In the structural design stage of the shells, these deformations must be interpreted as geometrical imperfections which can significantly reduce the high buckling resistance of the perfect geometry saddle shell.

After a brief introduction on the properties of cement composites and of GTR-IPC in particular, this paper presents a methodology to generate force-modelled anticlastic shell shapes that exploit both the tensile and compressive capacities of this composite. The shells are form found under self-weight using the dynamic relaxation method with kinetic damping. Application of the presented form finding methodology on four medium span (5–15 m) anticlastic shells explores the method's potential to develop structurally efficient anticlastic shell shapes experiencing mainly membrane action under their own weight, as demonstrated by finite element analysis of the case studies' structural behaviour under self-weight.

2. Textile reinforced cement composites (TRC)

2.1. Innovations in TRC: glass fibre textile reinforced inorganic phosphate cement

Nowadays, fibres are often used in concrete structures, be that plain or in combination with steel reinforcement. High performance fibre reinforced cement composites (HPFRCC) mix short fibres into a cement mortar or concrete, providing ductility to the brittle matrix. The limited tensile strength of HPFRCC [15] however restricts its application to structures carrying low tensile stresses, like thin wall cladding or façade renovation.

According to classic composite modelling, considerable amounts of fibres have to be inserted into the cementitious matrix in the direction of the tensile stresses to provide the necessary stiffness and strength beyond the introduction of multiple cracking in the matrix [16]. The development of Textile Reinforced Cement (TRC) composites addresses this need by impregnating continuous fibre systems, called textiles, with a cement or fine grained mortar. Whether containing continuous or discontinuous fibres, strictly aligned or randomly oriented, these continuous textiles provide a more orientation-controlled and significantly higher fibre volume fraction reinforcement for cement or concrete than discontinuous fibre systems such as in HPFRCC [8,9]. As in shells the stress directions vary with the applied loads, the used textiles are randomly oriented chopped fibre mats. The density of these textiles – and thus the fibre volume fraction and tensile capacity – that can be achieved depends on the maximum grain size and rheology of the cement matrix.

After more than ten years of study, researchers at the Vrije Universiteit Brussel developed a ceramic matrix, Inorganic Phosphate Cement [17], with a grain size ranging between 10 and 100 μm. Due to its relatively low viscosity of 2000 mPa s, dense glass fibre textiles can be impregnated by the matrix, leading to fibre volume fractions of more than 20% [10]. As the IPC matrix is pH neutral after hardening, cheaper E-glass fibres can be used instead of alkali resistant glass fibres necessitated for Ordinary Portland Cement based composites. Moreover, besides the composite hand lay-up manufacturing technique, an industrialised impregnation method, combining pressure and pultrusion techniques, was developed by Remy et al. [18] to reduce the production costs of this Glass fibre Textile Reinforced Inorganic Phosphate Cement (GTR-IPC). Producing and subsequently stacking individual laminates of 1 mm thickness, the shell thickness is well controlled during manufacturing and a low thickness tolerance (1 mm) can be assumed. Numerous building applications, such as sandwich panels for bridge design [19], hollow beams [9] and lightweight firewalls as shown in Fig. 1 [20], benefit from the structural yet fire resistant properties of this ceramic matrix composite.

Fig. 1. Lightweight GTR-IPC firewall.

2.2. Mechanical properties of glass fibre textile reinforced inorganic phosphate cement

Due to the small scale diameter as well as the random and homogeneous distribution of the reinforcement throughout the cement matrix, randomly oriented short glass fibre textile reinforced IPC (referred to as GTR-IPC) can be considered isotropic and homogeneous within a very small scale (approximately 1 cm) [8]. The composite possesses however a strong asymmetry in tensile and compressive behaviour. The constitutive behaviour of GTR-IPC under compression is mainly determined by the cement matrix and is approximately linear elastic. The Young's modulus in compression equals 18 GPa, and the compressive strength exceeds 50 MPa.

Its behaviour in tension however is highly nonlinear due to matrix crack initiation and propagation at very low stress levels. Fig. 2 shows the stress–strain curve of a 500 mm × 75 mm × 5 mm, 20 volume percent randomly oriented GTR-IPC specimen under increasing tensile load. Three stages can be distinguished in the tensile behaviour of GTR-IPC [21]:

Stage I: pre-cracking. At the beginning of loading, the stiffness of the uncracked composite is determined by the "law of mixtures" for linear elastic composites and is equal to the Young's modulus in compression (18 GPa). Since the volume fraction of the glass fibres is 20%, the matrix mainly determines the stiffness in this first stage.

Stage II: multiple cracking. When exceeding the tensile strength of the IPC matrix, the first cracks appear. At the crack face, the whole tension force has to be carried by the reinforcement. As the amount of fibres is larger than the critical fibre volume fraction, the acting load can be carried and the composite does not fail. As the tension force increases, additional cracks occur: due to the frictional bond between filaments and matrix, forces are transferred in the IPC matrix until its tensile strength is reached again. The cracking distance and the crack width are determined by the properties of the reinforcement, the bond characteristics between reinforcement and matrix, and the tensile failure strain of the matrix.

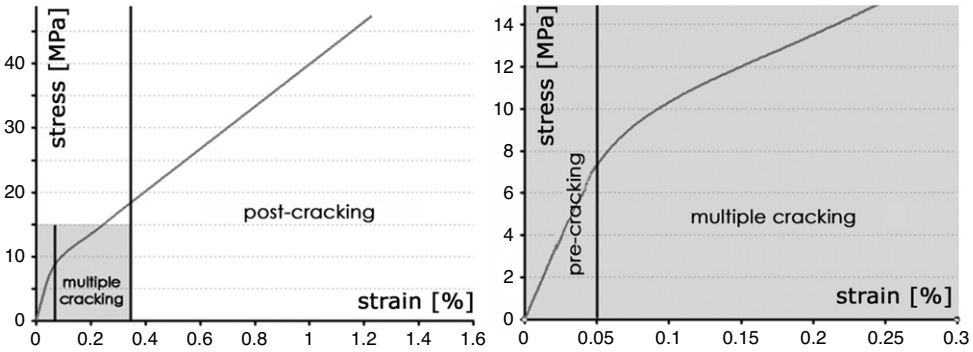

Fig. 2. Experimental stress–strain behaviour of 20 fibre volume% GTR-IPC under uniaxial tensile load.

Stage III: post-cracking. In this stabilised crack pattern stage, no further cracks occur. As the load increases, the filaments are strained further until their strength is reached. Failing of the specimen can however also happen as a result of fibre pull-out. The matrix stresses remain constant in this stage and only the fibres contribute to the composite's stiffness.

Due to the high fibre volume fraction, the composite's tensile strength reaches up to 48 MPa (see Fig. 2) and thus approaches the compressive strength of GTR-IPC. The tensile stiffness after cracking is lower than the compressive stiffness, but can still largely contribute to the structural behaviour of a tensed element. GTR-IPC represents thus a fire safe composite with high tensile as well as compressive capacities. Its extraordinary properties are used in this research to design tension and compression bearing, saddle shaped shells for building applications.

3. Form finding of anticlastic GTR-IPC shells using the dynamic relaxation method with kinetic damping

Material in a structural member is most efficiently used if the member experiences only membrane forces, and no bending. Typical structural systems that carry principal loads under membrane action only are either cables and membranes for pre-stressed structures, or catenary arches and shells for gravity loaded systems. Physical form finding experiments such as hanging chain models with weights, and their numerical equivalents, determine the shape for which the hanging chains – possessing no bending stiffness – are in equilibrium. In this way, optimal shapes are generated that upon inversion define pure compression shells under self-weight.

The presented research develops a form finding methodology to generate GTR-IPC shell surfaces subjected to both membrane actions (tension and compression) under self-weight. The method represents the continuous shell by a set of link elements (with only axial but no bending stiffness) for which the static equilibrium shape is determined under an applied load for a set of boundary conditions. Hence, the resulting shell shape experiences only membrane forces. The two most frequently used numerical form finding techniques to determine this equilibrium are the dynamic relaxation method [22,23] and the force-density method [24,25]. The presented shell form finding strategy uses dynamic relaxation with kinetic damping to determine the equilibrium of the gravity loaded system. The background of this method is discussed in paragraph 3.1. When altering the boundary conditions or the applied load, a different static equilibrium shape is obtained. Paragraph 3.2 presents how the boundary conditions can be manipulated to develop, with this numerical form finding method, anticlastic shell shapes in which both tension and compression occurs. Finally, paragraph 3.3 discusses the finite element modelling of these GTR-IPC shells, which allows the demonstration of the force-efficiency of the optimised shell shapes in the four performed case studies.

3.1. The dynamic relaxation method

The dynamic relaxation method [22,23] iteratively determines the static equilibrium of an initial arbitrary shell geometry created by a grid of links and nodes. The links are attributed a low elastic stiffness, the nodes' fictitious masses. Starting from this inaccurate and arbitrary specified geometry in the form finding process, application of gravity loads on the nodes causes an imbalance of internal and external forces which accelerates the nodes. The basis of the method is to follow the movement of each node of the grid from its initial unloaded position for small time intervals until an equilibrium shell shape is obtained under the applied loading. This time-incremental procedure can be summarised as follows:

(i) determination of the residual forces on the nodes of the current geometry, based on the external loads and internal forces in the current geometry;
(ii) calculation of the acceleration of every node by dividing the nodal residual forces by the nodal masses (using Newton's second law for motion);
(iii) integration of the acceleration over the next time step to determine the new nodal velocities;
(iv) integration of the nodal velocities over the next time step to obtain the new nodal displacements, which determine the new incremental geometry for which the internal forces and residual forces on every node are recalculated (i).

The presented dynamic relaxation method uses kinetic damping. The underlying basis of the kinetic damping concept is that as an oscillating body passes through a minimum potential energy state, its total kinetic energy reaches a local maximum. The method thus traces the relative displacement of the nodes until the kinetic energy of the system reaches a maximum. Then, all nodal velocity components are set to zero and the following iteration starts from this new geometry. This iterative process continues until all vibrations have died out and the shell structure converges to its static equilibrium shape.

Whereas for stress analysis the initial state is the equilibrium geometry and the effective material stiffness E and link element cross section A is attributed to the structure, the form finding procedure starts from an arbitrary geometry, and the elastic stiffness of the link elements can be used to control the shape. In the particular case of anticlastic shell design, the elastic stiffness is manipulated to control the sagging at the shell's midspan, as is shown in the various case studies in the following paragraphs.

3.2. Form finding methodology for force-modelled anticlastic TRC shells

3.2.1. Step 1: Analytical form finding of arch edges

The preliminary design of the TRC shell sets out the design limits (span, maximum and minimum heights) that need to be respected during the form finding process. In all four case studies, the shell consists of one or more saddle surfaces, pinned line-supported at the opposite side edges, and with unrestrained (vertical or inclined) arch edges at the other two opposite sides.

The first step in the form finding process consists of establishing the optimal catenary geometry of the arch edges under self-weight. This phase can be performed in any numerical form finding analysis or derived analytically. Due to the simplicity of this 2D problem, the arch shape is found analytically by inverting the shape of a freely hanging chain under self-weight. The catenary formula is:

$$z = \frac{T_0}{w} \cdot \cosh\left(\frac{w \cdot y}{T_0}\right) \tag{1}$$

where:

- y the horizontal and z the vertical coordinate of the arch in the y, z plane
- w vertical load equally distributed over the arch length, representing the self-weight per arch length
- T_0 horizontal component of the reaction force (and per definition equal to the horizontal component of the section force at any location on the catenary).

The ratio of the horizontal reaction force to the self-weight per unit arch length, T_0/w, completely defines the catenary's shape. This catenary formulation implies that the central point of the catenary does not pass the z-axis at its origin, but that $z = \frac{T_0}{w}$ if $y = 0$. From Eq. (1), using $z = \frac{T_0}{w} + H$ if $y = L$, the relation between the span $2L$ and the height H of the arch can be written as:

$$H = \frac{T_0}{w} \cdot \left[\cosh\left(\frac{w \cdot L}{T_0}\right) - 1\right]. \tag{2}$$

From this implicit equation, the value of T_0/w is determined that respects the arch span and height restrictions. Then the geometry of the catenary is determined with Eq. (1) and inverted. The inclined arches are found by rotation of the vertical inverted hanging catenaries.

3.2.2. Step 2: Numerical surface form finding between the restrained arch edges

The second step in the form finding process, the force modelling of the anticlastic shell surface, starts from an initial arbitrary shape. For convergence reasons and simplicity of input data, the initial shape is modelled as a single curved surface between the arch edges. A regular grid of nodes on this surface, connected by straight line elements (links) in both perpendicular directions of the anticipated compression and tension force lines, sets out the initial geometry. The links have no bending stiffness and can only carry normal forces (tension or compression).

The arch edges are pinned to respect the geometry of the boundaries and to provide tensile resistance to the link elements in the direction of the hanging catenaries. The line supports at the bottom are not restricted, leading to line elements in tension during the form finding process. However, in reality the bottom edges are pin supported, leading to compression in the direction of the arches that compose the surface. In all nodes, a load conforming to 20 mm GTR-IPC self-weight is applied. As a fictitious axial stiffness will be applied to the link elements, the magnitude of the force is not important, yet its distribution must represent the self-weight of the shell (equal distribution over the curved surface area).

Attributing a small, fictitious and solely axial stiffness EA to the link elements, the static equilibrium under self-weight found with the dynamic relaxation method is the optimised curved grid that holds the continuous shell surface and experiences exclusively membrane action. The shell's equilibrium shape depends on this fictitious axial stiffness EA: the lower its value, the larger the displacement of the free nodes from their original position, and the lower the lowest sagging point at the anticlastic shell's midspan for a fixed loading condition. As this midspan height is *a priori* fixed by the design requirements, the axial stiffness of the linked elements is varied iteratively until the required midspan height is obtained. In the case of convergence problems, a first iteration with a larger axial stiffness can be performed, after which its new geometry – closer to the final shape – is used as initial input geometry for a second form finding procedure.

3.2.3. Step 3: From grid surface to continuous shell surface

The use of a grid-based form finding method for continuous shells has the disadvantage that the continuous shell must be formed through the discrete grid structure. In this study, the continuous shell is found by creating splines through the optimised position of the nodes in both perpendicular directions, and subsequently filling the grid structure existing of curved hanging catenaries and arches by minimal surface areas. Cutting the sagging bottom side edges assures a level connection with the external supports at ground level.

3.3. Verification under self-weight

Finite element analysis using the commercially available software package Abaqus (version 6.8-1) verifies the structural behaviour of the designed anticlastic shell shapes under self-weight. Moreover these case studies demonstrate the validity of the proposed form finding methodology. The shells are modelled with 8 node quadrilateral thin shell elements with five degrees of freedom per node (three displacements and two in-surface rotations). GTR-IPC is modelled isotropically on a macro scale. Table 1 summarises the used material properties of 20 fibre volume percent GTR-IPC. Even though the tensile strength of GTR-IPC approaches its compressive strength, the composite's tensile stiffness reduces significantly after matrix multiple cracking. Therefore equal axial stiffness in compression and tension can only be assumed if the tensile stresses experienced under self-weight remain in the linear elastic stage. For all case studies it is therefore verified whether the maximum tensile stress does not exceed the matrix cracking stress (7 MPa).

Table 1
Material properties of 20 fibre volume% TRC.

Matrix	Inorganic Phosphate Cement (IPC)		
Fibre textile	*E*-glass fibres		
Fibre volume fraction	V_f	%	20
Density	ρ	kg/m^3	1900
Initial *E*-modulus	E_1	GPa	18
Poisson coefficient	υ		0.3
Cracking stress	σ_{crack}	MPa	7

4. Case study 1: anticlastic shell covering a 10 m × 10 m area

The first case study consists of one saddle shaped shell covering a square area of 10 m by 10 m. The free, vertical arch edges span 10 m with a maximum height of 5 m. The whole 10 m long bottom side edges are pinned. The final surface must have a fixed midspan height of 2.85 m.

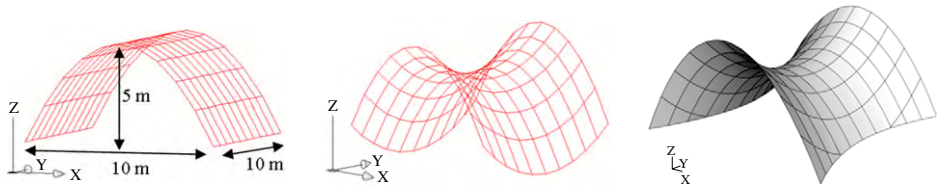

(A) Initial geometry. (B) Anticlastic grid geometry after form finding. (C) Continuous shell after form finding.

Fig. 3. Form finding evolution of case study 1.

4.1. Form finding

The shell initially is modelled as a singly curved grid surface between 5 m tall catenary arches (as shown in Fig. 3(A)). 10 × 10 straight link elements discretise this initial surface. Mesh refinement demonstrated that this number of link elements assures computational convergence (i.e. the difference in optimal node coordinates between a shell modelled with 20 × 20 link elements and with 10 × 10 link elements was far inferior to 1%). During the surface form finding, the arches are pinned to provide tensile resistance to the tension catenaries that will develop between them; the bottom side edges are free. External gravity loads equivalent to the self-weight of a 20 mm thick shell are applied in every node. With an elastic stiffness, *EA*, equal to 20 kN in all link elements, the anticlastic shell comes to a static equilibrium shape in the form finding process that respects the 2.85 m central height restriction. Fig. 3(B) shows the force-modelled anticlastic grid shell, completely in tension under the form finding boundary conditions. In reality however, the arch edges will be released while the lower side edges will be restrained, leading to a shell with compression arches between the side edges, and perpendicularly hanging catenaries in tension between the arches. Fig. 3(C) shows the continuous shell, created by minimal surfaces between two orthogonal sets of splines through the nodes, and with external ground level supports.

4.2. Structural analysis

Limit state design of the considered case study was part of the previously published research by the authors [13] and proved that an overall shell thickness of 20 mm is sufficient to resist deformations, stresses and buckling under self-weight, wind and snow loads. Buckling analysis showed that the critical buckling load of the 20 mm thick shell exceeds nine times the most disadvantageous load combination. This large safety factor accounts for the possible reduction of the perfect shell's buckling load due to imperfections caused during manufacturing (deformation of fabric formwork, small local variations of thickness and composite's fibre volume fraction). A constant thickness of 20 mm is therefore attributed to the shell. The shell is pinned along the bottom side edges and loaded under self-weight only. The applied GTR-IPC material parameters are summarized in Table 1. 40 × 40 thin shell elements (described in Section 3.2) ensure computational convergence in the structural finite element analysis.

First indicators of the validity of the proposed shell form finding methodology are the very low displacements and stresses under self-weight. The maximum total displacement amounts to 0.27 mm, and the maximum vertical displacements equal 0.12 mm downward (near the corners) and 0.088 mm upward (centre of the shell). Maximum compressive stresses (0.31 MPa) occur near the corners; maximum tensile stresses are even lower (0.08 MPa). As tensile stresses remain largely under GTR-IPC's cracking stress (7 MPa), the assumption of equal elastic stiffness in tension and compression is valid.

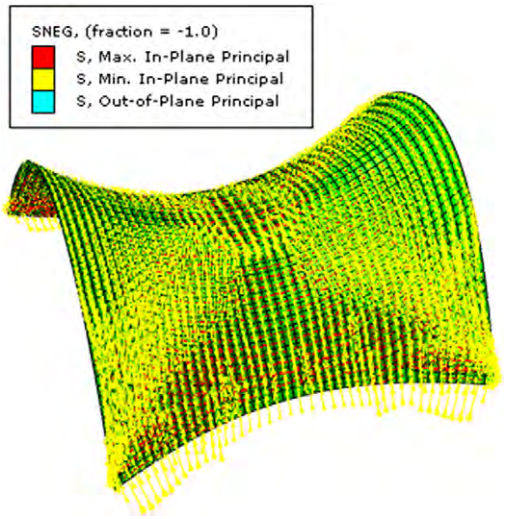

Fig. 4. Principal, in plane stress vectors in shell case study 1, under self-weight.

A vector plot of the stresses in the bottom surface (Fig. 4, similar stresses occur in the top surface) shows how compressive stresses (yellow vectors) follow the direction of the arch lines that constitute the surface, as anticipated by the form finding method. However, as the unrestrained arch edges do not provide enough tensile resistance, the tensile stresses (red vectors in Fig. 4) in the hanging catenary direction are low and decrease from the bottom sides of the shell to halfway the span.

5. Case study 2: anticlastic shell with overhangs

Case study 2 studies the effect of overhangs on the structural behaviour of the anticlastic shell under self-weight by adding 1 m long overhangs at both free arch edges of case study 1. The new inclined arch height, 5.95 m, is determined by extending the midspan hanging catenary of case study 1 over 1 m length at both sides. This assures the shape similarity of case studies 1 and 2. The anticlastic shell has thus a maximum width of 12 m, a maximum height of 5.95 m, and spans 10 m by 9.5° inclined planar arches.

5.1. Form finding

The inversion of a 6 m high, vertical, hanging chain and its subsequent rotation over 9.5° determines the geometry of the inclined boundary arches. Between these arches, 12 × 10 link elements create the start geometry of the grid shell (Fig. 5(A)). The surface form finding method is equal to case study 1: the inclined edges are pinned, the bottom side edges are free. Under self-weight, the surface relaxes to a stable equilibrium with the centre point at 2.85 m height if the links have an elastic stiffness, *EA*, of 14 kN. As the nodes in the form found geometry lie further from their initial position as in the first case study, the elastic stiffness to obtain the predefined central height is obviously smaller. Fig. 5(B)

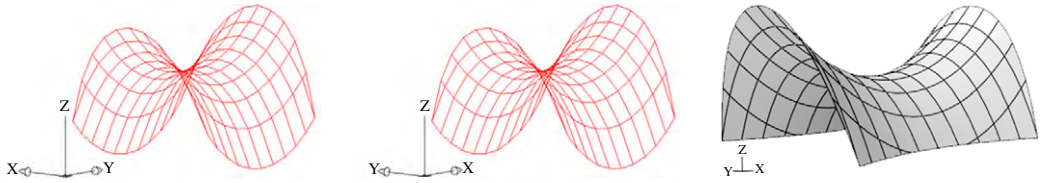

(A) Initial geometry. (B) Anticlastic grid geometry after form finding. (C) Continuous shell after form finding.

Fig. 5. Form finding evolution of case study 2.

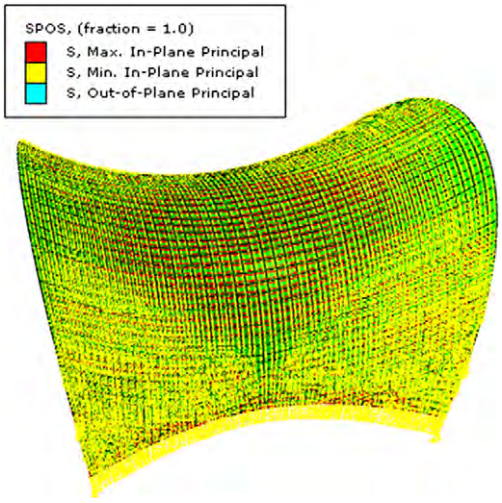

Fig. 6. Principal, in plane stress vectors in shell case study 2, under self-weight.

and (C) show the geometry of the optimised grid and continuous shell respectively.

5.2. Structural analysis

Due to equivalency with the previous case study, the shell is attributed the same shell thickness, namely 20 mm. It is however clear that this is only a preliminary shell thickness; limit state design of this shell – with different geometry and thus different structural behaviour than case study 1 – is absolutely necessary in the successive design stage. For the verification of the form finding method by analysis of the structural behaviour of the shell under self-weight loading, however, the load pattern (distributed self-weight loading) is of importance rather than the magnitude of the load. The stress vectors in the top shell surface (Fig. 6, similar for bottom surface) demonstrate the significantly different structural behaviour, under self-weight, of the anticlastic shell with overhangs. As the overhang tends to move downward under its self-weight, the catenaries hanging between the arches are stressed in tension. This phenomenon is obviously most present towards the middle of the span. In the perpendicular direction, self-weight is carried by arch action. The interaction of hanging catenaries in tension and arches in compression carries external loads to the supports. This behaviour reflects the well-known membrane action of hypar shells, and exploits the tensile material capacities of TRC.

The lower maximum displacements confirm the improved structural behaviour under self-weight with reference to case study 1. The maximum total displacement amounts to 0.12 mm instead of 0.27 mm. In the vertical direction, the shell only moves downwards to 0.098 mm instead of both upwards (0.088 mm) and downwards (0.12 mm). The maximum compressive (0.31 MPa) and tensile (0.048 MPa) stresses both validate the assumption of equal elastic stiffness in tension and compression, and prove the efficiency of the shell to carry its own weight.

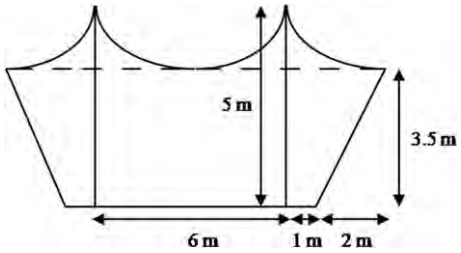

Fig. 7. Side elevation of preliminary design case study 3.

6. Case study 3: shell composed of three anticlastic parts

A continuous composition of three consecutive anticlastic shapes forms the subject of the third case study. Fig. 7 shows the side elevation and dimensions of the shell's preliminary design. This geometry is unprecedented for traditional steel-reinforced concrete shells. Tensile structures with this shape are common, but are anchored to boundary arches to obtain structural stiffness. The central anticlastic part has a length of 6 m, a central height of 3.5 m and ends at 5 m high vertical arches. Anticlastic forms hang from both arches, decreasing in height to 3.5 m at the centre of the shell edge. The planar arch edges are inclined 30° from the vertical. The shell has a total length of 12 m and spans 10 m across. The shell's 8 m long bottom sides are pinned.

6.1. Form finding

First, inversion of a freely hanging chain lays out the optimal shape under self-weight of both the internal and the external arches. The external arches are then rotated over 30° from the vertical. Linearly increasing in height between the four arches, straight link elements create the initial rectangular grid geometry as shown in Fig. 8(A). Only the internal and external arches, already optimised in shape for the postulated span and height, are pinned during form finding of the shell surface. In reality however, these arches will be free, while the bottom side edges will be pin supported. Under 20 mm thick equivalent self-weight load and with an elastic link stiffness of 7.8 kN, the height at the shell's centre – set in the preliminary design (Fig. 7) – equals the central height of the inclined arches, namely 3.5 m. Fig. 8(B) shows the static equilibrium shape resulting from the dynamic relaxation process. Fig. 8(C) depicts the continuous shell with levelled bottom edges.

6.2. Structural analysis

In order to study the shell's structural behaviour under self-weight and herewith the validity of the form finding methodology on this case study, the shell thickness is set equal to that of case study 1, namely 20 mm. This is only a preliminary thickness in this shape optimisation design stage; future limit state design of this shell is necessary to determine its design thickness (as was

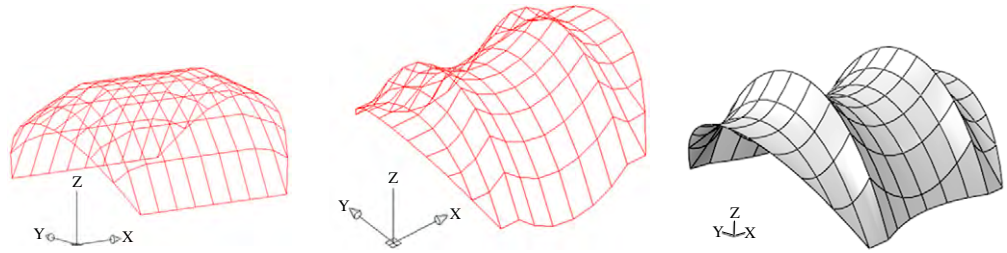

(A) Initial geometry. (B) Anticlastic grid geometry after form finding. (C) Continuous shell after form finding.

Fig. 8. Form finding evolution of case study 3.

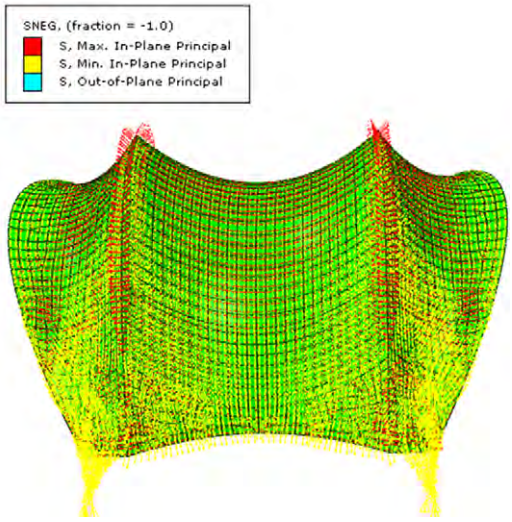

Fig. 9. Principal, in plane stress vectors in shell case study 3 under self-weight.

performed for case study 1 in [13]). Pinned supports restrain the entire length of the bottom edges while the arches are free.

The finite element analysis shows that mainly membrane forces carry the shell's self-weight. At the inner arches, small bending moments occur. The displacements in the middle shell part are also very small. The largest displacements ($U_{max} = 0.38$ mm, $U_{z,max} = 0.30$ mm upwards) take place near the bottom corners. Fig. 9 shows the tensile stress vectors in the hanging catenary direction and compressive stress vectors in the arch direction. The self-weight of the overhangs causes these tensile stresses in the shell. Though relatively small, maximum tensile (0.32 MPa) and compressive (0.66 MPa) stresses concentrate at the sharp transitions between two consecutive shell parts, and near the corners. Thickening and/or smoothing of these discontinuities in the shell surface, as well as thickening of the bottom edges, could reduce even more the stresses and displacements of the structure.

7. Case study 4: asymmetrical shell with overhangs

Practically unlimited in its thickness, GTR-IPC presents the optimal cement composite for thin shell applications. Pre-fabricated on a membrane formwork, mass-produced anticlastic TRC shells are an economical alternative for small spans such as bus stands, bicycle racks, small train stations etc.

The anticlastic shell in case study 4 spans 5 m and has a total length of 2.5 m. Due to its envisioned asymmetrical applications (i.e. main opening of bus stand or bicycle shelter towards the road), the design itself is also asymmetrical: in the length direction, the shell is composed of a central, 1 m long bottom edge pinned at ground level with on the one side a main overhang of 1 m long and 4 m high, and on the other side a secondary overhang of 0.5 m long and 3.25 m high.

The span of 5 m and a central height of 2.75 m assures a free box space of 2 m wide, 2.5 m long and 2.2 m high. With these dimensions, the shell is transportable and complies with the Belgian unexceptional transport regulations [26].

7.1. Form finding

Firstly, 5 m spanning hanging chains with a height of 4.12 and 3.28 m are inverted and rotated 14° and 8.75° from the vertical respectively to create the 4 and 3.25 m high arch edges. These boundaries are pin-supported during the shell surface form finding process to support tensile forces in the catenaries hanging between them. The central one meter long bottom side edges are unrestrained. Two perpendicular sets of straight link elements between these four edges define the grid geometry before surface form finding (see Fig. 10(A)). For an elastic stiffness of 0.3 kN, the equilibrium structure loaded by 10 mm thick GTR-IPC self-weight respects the *a priori* imposed central height restriction of 2.75 m (Fig. 10(B) and (C)).

7.2. Structural analysis

As the span of the studied shelter is only half of the span in case study 1 (5 m instead of 10 m), a preliminary thickness of 10 mm is attributed to the shell in this shape optimisation design stage. An iterative study under self-weight shows that thickening of the 0.5 m long secondary overhang up to 30 mm counterbalances the rotational moment of the larger primary overhang. In this way, the asymmetrical shell only introduces compressive forces into the external ground level supports.

Fig. 11(A) and (B) show the tensile (red) and compressive (yellow) stress vectors in the top and bottom shell surface respectively. Due to the relatively large overhangs, the self-weight is not only carried by hanging tensile catenaries and compression arches like in previous case studies, but also small, local, bending moments occur. However, the small maximum displacements (0.41 mm) and stresses (0.27 MPa in tension and 0.30 MPa in compression) show that the proposed method is also useful to minimise the bending inevitably occurring in shells with large overhangs.

8. Conclusions

The reinforcement of a very fine grained Inorganic Phosphate Cement (IPC) with glass fibre textiles creates a new material, GTR-IPC, which resembles polymer matrix composites from a mechanical point of view, but is fire-resistant like concrete. With this innovation in composite technology, new possibilities for shell structures arise. GTR-IPC shells covering medium spans (up to 15 m) can have a reduced thickness and are thus much lighter in

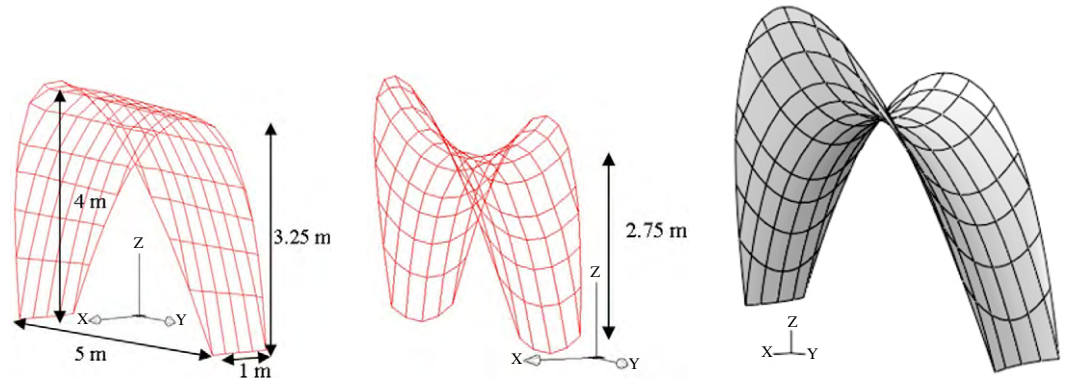

(A) Initial geometry. (B) Anticlastic grid geometry after form finding. (C) Continuous shell after form finding.

Fig. 10. Form finding evolution of case study 4.

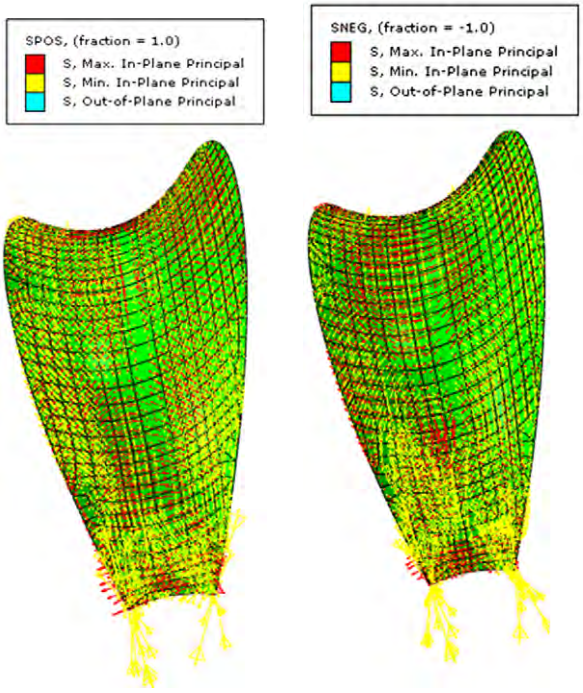

(A) Top surface. (B) Bottom surface.

Fig. 11. Principal, in plane stress vectors in shell case study 4 under self-weight.

comparison to steel-reinforced concrete shells. This paper focuses on the form finding of anticlastic shell shapes which exploit both the tensile and compressive capacities of GTR-IPC.

A form finding methodology, using the dynamic relaxation method, describes the process to generate force-modelled anticlastic TRC shells carrying their self-weight through membrane action only, by the joint effort of catenaries in tension and in compression. The design methodology is illustrated by four case studies and validated by the finite element analysis of their structural behaviour under self-weight.

Conclusively, the research presented in this paper demonstrates how renewing thin shell designs, unseen for steel-reinforced concrete shells for such small spans, can be found with the presented methodology, taking advantage of the exclusive mechanical properties of textile reinforced cement composites. The combination of cement composites and fabric formwork innovation open a whole new range of shell designs and applications, to be explored in the future.

Acknowledgments

This research is financially supported by the Fund for Scientific Research in Flanders, Belgium (FWO), through a scholarship and a travel grant to Princeton University (USA) for the first author.

References

[1] Espion B, Halleux P, Schiffmann JI. Contributions of André Paduart to the art of thin concrete shell vaulting. In: Huerta S, editor. Proceedings of the 1st international congress on construction history. 2003. p. 829–38.
[2] Teng JG, Wong HT, Wang ZC, Dong SL. Large-span steel–concrete composite shell roofs. In: Proceedings of the international. Symposium on innovation and advances in steel structures. 2004.
[3] West M. Thin-shell concrete from fabric moulds. Manitoba: Centre for Architectural Structures and Technology; 2006.
[4] Pronk A, Houtman R, Afink M. The philips pavilion. In: New olympics, new shell and spatial structures, proceedings of the international association for shell and spatial structures. IASS. Symposium. 2006. p. 508 and paper ref. MO20 [cd-rom].

[5] Cauberg N, Parmentier B, Vanneste M, Mollaert M. Shell elements of architectural concrete using fabric formwork—part 1: concept. In: Oehlers DJ, Griffith MC, Seracino R, editors. Proceedings of the international symposium on fibre-reinforced polymer reinforcement for concrete structures. FRPRCS-9, 2009. p. 53–4. and [cd-rom].
[6] Guldentops L, Mollaert M, Adriaenssens S, De Laet L, De Temmerman N. Textile formwork for concrete shells. In: evolution and trends in design, analysis and construction of shell and spatial structures, proceedings of the international association for shell and spatial structures. IASS. Symposium. 2009. p. 406–7 and 1743–1754 [cd-rom].
[7] Chilton J. 39 etc. . .: Heinz Isler's infinite spectrum of new shapes for shells. In: Evolution and trends in design, analysis and construction of shell and spatial structures, proceedings of the international association for shell and spatial structures. IASS. Symposium. 2009. p. 58–9 and 51–62 [cd-rom].
[8] Cuypers H, Wastiels J. Thin and strong concrete composites with glass textile reinforcement: modeling the tensile response. In: Dubey A, editor. SP-250 textile reinforced concrete. 2008. p. 131–48. paper ID: SP-250-10 [cd-rom].
[9] Promis G, Gabor A, Maddaluno G, Hamelin P. Behaviour of beams made in textile reinforced mineral matrix composites, an experimental study. Compos Struct 2010;92(10):2565–72.
[10] Remy O, Wastiels J. High performance textile reinforced cements: tensile hardening behaviour and modelling. In: Marques A, Juvandes L, Henriques A, Faria R, Barros J, Ferreira A, editors. Proceedings of the international conference on challenges for civil construction. CCC. 2008. p. 116–7. and [cd-rom].
[11] European Committee for Standardisation. Eurocode 2: design of concrete structures—part 1–1: general rules and rules for buildings: 4: durability and cover to reinforcement. CEN. 2004.
[12] Tysmans T, Adriaenssens S, Cuypers H, Wastiels J. Structural analysis of small span textile reinforced concrete shells with double curvature. Compos Sci Technol 2009;69(11–12):1790–6.
[13] Tysmans T, Adriaenssens S, Wastiels J. Shape optimization of small span textile reinforced cementitious composite shells. In: Evolution and trends in design, analysis and construction of shell and spatial structures, proceedings of the international association for shell and spatial structures. IASS. Symposium. 2009. p. 408–9 and 1755–1766 [cd-rom].
[14] Holgate A. The art of structural engineering: the work of Jörg Schlaigh and his team. Stuttgart (London): Axel Menges; 1997.
[15] Reinhardt HW, Naaman AE, editors. High performance fibre reinforced cement composites. Proceedings of the 5th international RILEM workshop. HPFRCC5, 2007. p. 1–134.
[16] Aveston J, Cooper GA, Kelly A. Single and multiple fracture. In: The properties of fibre composites. Proceedings of the conference national physical laboratories. London: IPC Science & Technology Press Ltd.; 1971. p. 15–24.
[17] EP 0 861 216 B1. Inorganic resin compositions. Their preparation and use thereof.
[18] Remy O, Wastiels J. Development of an impregnation technique for glass fibre mats to process textile reinforced cementitious composites. Plast Rubber Compos 2010;39(3–5):195–9.
[19] Giannopoulos G, Vantomme J, Wastiels J, Taerwe L. Construction and experimental analysis of a pedestrian bridge with concrete deck and IPC truss girder. Sci Eng Compos Mater 2004;11(1):8–18.
[20] Hiel C. Improving the reliability of the electric grid infrastructure: case study of firewalls manufactured with fiber reinforced inorganics (FRI). In: Proceedings of the American society for composites. 2009. p. 14 [cd-rom].
[21] Hegger J, Will N, Bentur A, Curbach M, Jesse F, Mobasher B, Peled A, Wastiels J. Mechanical behaviour of textile reinforced concrete. In: Brameshuber W, editor. Textile reinforced concrete: state of the art report of RILEM technical committee 201-TRC. Bagneux (France): RILEM Publications; 2006. p. 29–35. 135–147.
[22] Barnes MR. Form-finding and analysis of tension structures by dynamic relaxation. Int J Space Struct 1999;14(2):89–104.
[23] Adriaenssens SML, Barnes MR. Tensegrity spline beam and grid shell structures. Eng Struct 2001;23(1):29–36.
[24] Schek HJ. The force density method for form finding and computation of general networks. Comput Methods Appl Mech Engrg 1974;3(1):115–34.
[25] Linkwitz K. About formfinding of double-curved structures. Eng Struct 1999; 21(8):709–18.
[26] Goldstein GE, Labeeuw G. Handleiding van de atlas der reiswegen voor uitzonderlijk vervoer en havenfiches. In: Federaal ministerie van verkeer en infrastructuur. MVI—ACI—directie wegen. 2001. p. 1–3.